

Theory of Antiferromagnetic Correlations and Neutron-Scattering Cross Section in Heavy-Fermion Metals

A. Auerbach, Ju H. Kim, and K. Levin

The University of Chicago, James Franck Institute, Chicago, Illinois 60637

and

M. R. Norman

Materials Science Division, Argonne National Laboratory, Argonne, Illinois 60439

(Received 6 August 1987)

We show that antiferromagnetic correlations with frequencies scaling as the inverse mass enhancement are universal features of coherent heavy fermions. The associated neutron cross-section peaks may be either quasielastic or inelastic. Spin-orbit and crystal-field interactions yield zone-center peaks at comparable frequencies. This experimentally observed behavior is derived from a $1/N$ expansion. Because these correlations are not "soft" and are general features of hybridized band structure, they do not necessarily elucidate the superconducting mechanism.

PACS numbers: 75.30.Mb, 71.28.+d, 75.20.Hr, 75.50.Ee

Important insight into the nature of heavy-fermion compounds is provided by observations of scaling behavior in the resistivity, specific heat, and susceptibility in the low-temperature coherent regime.¹ To be added to this list of "universal" thermodynamic properties is the structure of the low-temperature neutron cross section,²⁻⁴ which reveals inelastic antiferromagnetic peaks in the dynamical susceptibility at millivolt frequencies in at least three heavy-fermion materials: UPt₃, CeCu₆, and UBe₁₃. Equally general is the behavior of the zone-center contribution which, contrary to simple one-component Fermi-liquid theories, also exhibits a peak at comparable frequencies.

It is the purpose of this paper to address these neutron data within the same theoretical framework⁵ which has been successfully applied to study the various thermodynamical properties noted above. Our starting point is the Anderson lattice model properly modified to include

spin-orbit effects. While we will confine our specific calculations to the $1/N$ framework (where N is the degeneracy of the f level), *we stress that our physical interpretation is more general.*

The calculation of the neutron cross section relates to two very central issues in heavy-fermion materials: (1) the role that the observed antiferromagnetic fluctuations play in mediating the superconductivity and (2) the widely held view^{2,6} that a picture based on a Fermi liquid of band quasiparticles cannot explain neutron data in heavy-fermion systems which have been analyzed primarily in terms of Kondo impurity models or localized f spins. These interpretations of neutron experiments seem to be at odds with the extensive experimental evidence⁷ for coherent transport and itinerant f electrons.

We assume that the Hamiltonian describing Ce- and U-based heavy-fermion compounds is given by the extended Anderson lattice model

$$H = \sum_{\mathbf{k},s} \epsilon_{\mathbf{k}} c_{\mathbf{k}s}^{\dagger} c_{\mathbf{k}s} + \sum_{i,m} (\epsilon_f f_{im}^{\dagger} f_{im}) + \frac{V}{\sqrt{N}} \sum_{\mathbf{k},i,s,m} \{e^{i\mathbf{k}\cdot\mathbf{r}} u_{s,m}(\mathbf{k}) c_{\mathbf{k},s}^{\dagger} f_{i,m} + \text{H.c.}\} + U \sum_{i,m \neq m'} f_{im}^{\dagger} f_{im} f_{im'}^{\dagger} f_{im'}, \quad (1)$$

where $\epsilon_{\mathbf{k}}$, ϵ_f , and V are the conduction-band, valence-band, and hybridization energies, respectively.⁸ Here U is the large Coulomb repulsion. The spin indices m and s run over the crystal-field levels and conduction-electron-spin states, respectively. Their degeneracy is given by the same number N . In the limit of large mass enhancement, the electronic energy $T_{\mathbf{k}}$ is much smaller than the lowest crystal-field splitting Δ . Thus only the lowest Kramers doublet in Eq. (1) needs to be retained and the contribution of the higher crystal-field levels to Van Vleck paramagnetism⁸ can be ignored. While these arguments require that $N=2$, we will treat N as a general parameter. The pseudospin matrices $u_{s,m}(\mathbf{k})$ represent the scattering amplitude of a conduction electron

from this doublet. We assume they have the same functional form as in Ref. 8 with only the lowest doublet included.

In the limit of infinite U and large N , it is well known that within mean-field theory [$O(1/N)^0$], Eq. (1) leads to quasiparticles described by two hybridized bands with energies $E_{\mathbf{k}}^{\alpha}$, $\alpha=1,2$. As a result of infinite U the f level is raised slightly above the Fermi level, and the hybridization is severely reduced, thus leading to the large effective mass $m^*/m \sim \gamma \alpha T_{\mathbf{k}}^{-1} \gg 1$, where γ is the linear coefficient of the specific heat. Interactions between the quasiparticles⁵ appear at the next order in $1/N$. These interactions derive from correlated site-to-site fluctua-

tions, described by the 2×2 matrix propagator $D_{rr'}(\mathbf{q}, \omega)$, in the f level ($r=2$) and hybridization ($r=1$). An important consequence of this "Kondo boson" theory^{1,5} is that it contains a *single* energy scale T_K which characterizes both the electronic and boson energies. Because it is consistent with experimentally observed scaling

properties,¹ the $1/N$ approach (although $N=2$ is not large) is believed to represent the essential physics of the heavy Fermi liquids far from any instabilities.⁹

Inelastic neutron experiments measure the dynamical susceptibility which is dominated by that of the f electrons. In the present expansion the mean-field $O(1/N^0)$ term is given by the usual "bare" bubble diagram,

$$\chi_{MF}(\mathbf{q}, \omega) = - \sum_{\mathbf{k}Q\alpha\alpha'} \text{Tr}[(\mu_{\mathbf{k}\mathbf{k}+\mathbf{q}}^{\alpha\alpha'})^2] [f(E_{\mathbf{k}}^{\alpha}) - f(E_{\mathbf{k}+\mathbf{q}}^{\alpha+Q})] / (E_{\mathbf{k}}^{\alpha} - E_{\mathbf{k}+\mathbf{q}}^{\alpha+Q} + \omega + i\eta), \quad (2)$$

where the trace is over matrix elements of the electronic magnetic moment μ in the quasiparticle basis. The k, α dependence is through the coherence factors weighted by the appropriate g factors for the conduction (c) and f electrons. \mathbf{Q} represents all reciprocal lattice vectors. $\text{Im}\chi_{MF}$ vanishes at $\mathbf{q}=0$ for finite $\omega < \Delta$. However, the $O(1/N)$ contribution to $\text{Im}\chi(0, \omega)$ does not vanish and is analytically tractable. By inclusion of bubbles with all single exchanges of the Kondo-boson propagator, both self-energy (SE) and vertex (V) contributions to $\chi_{1/N} \equiv [\chi_{SE} + \chi_V]/N$ may be written as

$$\chi_{SE}(\bar{\omega}) = \sum_{[a], k, \kappa \pm rr'} \text{Tr}[\mu_{\mathbf{k}\mathbf{k}}^{\alpha\alpha'} \mu_{\mathbf{k}\mathbf{k}}^{\alpha''\alpha''}] G_{\mathbf{k}}^{\alpha'} G_{\mathbf{k}}^{\alpha''} G_{\mathbf{k}+\kappa}^{\alpha''} G_{\mathbf{k}+\bar{\omega}}^{\alpha} C_r^{\alpha'\alpha''} C_{r'}^{\alpha''\alpha} D_{rr'}(\kappa), \quad (3)$$

$$\chi_V(\bar{\omega}) = \sum_{[a], k, \kappa, rr'} \text{Tr}[\mu_{\mathbf{k}\mathbf{k}}^{\alpha\alpha'} \mu_{\mathbf{k}+\kappa, \mathbf{k}+\kappa}^{\alpha''\alpha''}] G_{\mathbf{k}+\bar{\omega}}^{\alpha} G_{\mathbf{k}}^{\alpha'} G_{\mathbf{k}+\kappa}^{\alpha''} G_{\mathbf{k}+\bar{\omega}}^{\alpha''} C_r^{\alpha\alpha'} C_{r'}^{\alpha''\alpha} D_{rr'}(\kappa). \quad (4)$$

We use a four-vector notation for k, q , and $\bar{\omega} = (0, i\omega_n)$. G^a are the mean-field Green's functions. Here, C_r are momenta-dependent coherence factors⁵ which couple the Bose propagator $D_{rr'}$ to the quasiparticles. Writing products of two Green's functions as their difference and dropping interband terms which are small for $\omega < \Delta$, we find for the zero-temperature limit

$$\text{Im}\chi_{1/N}(0, \omega) = \frac{2}{N} \sum_{\mathbf{q}} \int_0^{\omega} \frac{d\omega'}{\pi\omega^2} \text{Tr}[\bar{\Pi}''(\mathbf{q}, \omega') D''(\mathbf{q}, \omega - \omega')], \quad (5)$$

where we have traced over the boson indices r, r' and

$$\bar{\Pi}_{rr'}(\mathbf{q}, \omega) = - \sum_{\kappa\alpha\alpha'} \text{Tr}[(\mu_{\mathbf{k}\mathbf{k}}^{\alpha\alpha'} - \mu_{\mathbf{k}+\mathbf{q}, \mathbf{k}+\mathbf{q}}^{\alpha'\alpha'})^2] \frac{f(E_{\mathbf{k}}^{\alpha}) - f(E_{\mathbf{k}+\mathbf{q}}^{\alpha'})}{E_{\mathbf{k}}^{\alpha} - E_{\mathbf{k}+\mathbf{q}}^{\alpha'} + \omega + i\eta} C_r^{\alpha\alpha'} C_{r'}^{\alpha'\alpha}. \quad (6)$$

Here we have used the spectral representations for $\bar{\Pi}_{rr'}$ and $D_{rr'}$ to perform the Matsubara summations which introduces the imaginary parts of $\bar{\Pi}$ and D denoted by $\bar{\Pi}''$ and D'' , respectively. Equation (5), which is one of the central results of our calculations, is thus a closed-form expression for the leading-order contribution to the susceptibility at the zone center.

In a spin-conserving Fermi liquid, $\text{Im}\chi(0, \omega) = 0$ for $\omega \neq 0$. This is consistent with Eqs. (5) and (6) and can be explicitly deduced in the standard Anderson model [based on Eq. (1) with $u_{s,m}(\mathbf{k}) = \delta_{s,m}$]. A finite-frequency zone-center contribution to $\text{Im}\chi(0, \omega)$ reflects the fact that the magnetization is not conserved. While there is a weak effect ($\sim m/m^*$) deriving from the different g factors for the f and c electrons, the dominant contribution arises from the strong spin-orbit and crystal-field effects. This should be contrasted with the single-impurity case where the finite lifetime of the Kondo resonance causes f -spin dissipation. To make further progress in evaluating $\text{Im}\chi(0, \omega)$ we note from Eq. (6) that the magnetic-moment trace can be roughly approximated¹⁰ by a prefactor $\bar{\mu}^2(\bar{\mathbf{q}}) \{1 - \exp[-|\bar{\mathbf{q}}|/q]\}$, where $\bar{q} \sim 2k_F/3$. With use of parabolic bands the remaining integrals in $\bar{\Pi}$ and D are reduced to one dimension and performed numerically.

The numerically obtained behavior of the mean-field susceptibility [Eq. (2)] for both spherical and tight-

binding conduction-band structures in simple cubic Brillouin zones is as follows:

(I) For small Fermi surfaces, $\text{Im}\chi(q, \omega)$ is dominated by intraband transitions in the lower bands. These give the largest contribution at the zone boundary (and for $\omega \sim T_K$) since large wave vectors will maximize the phase space available for scattering to empty heavy-electron states across the Fermi surface. This behavior is illustrated in Fig. 1 in which is plotted $\text{Im}\chi_{MF}(q, \omega)/\chi_0$ for a simple cubic *tight-binding* conduction band as a function of ω in the $(0, q, q)$ direction at $T = T_K/5$ and $k_F = \frac{1}{3}\sqrt{3}\pi/a^*$ (a^* is the rare-earth separation). The frequency dependence can be described by a Lorentzian:

$$\text{Im}\chi = 2\chi_m \Gamma(\omega - \omega_0) / [(\omega - \omega_0)^2 + \Gamma^2], \quad \omega > \omega_0, \quad (7)$$

where χ_m , Γ , and ω_0 parametrize the peak's height, width, and threshold values. In case I the Lorentzian is quasielastic, defined by Eq. (7) with $\omega_0 = 0$.

(II) For large Fermi surfaces, $\text{Im}\chi(q, \omega)$ is dominated by interband transitions between regions of large density of states at the zone center and zone boundary.¹¹ This antiferromagnetic behavior is similar to that of case I and is shown in Fig. 2 for a *spherical* conduction band and $k_F = (3/2)^{1/2}\pi/a^*$ with $T = T_K/5$. In contrast to case I, however, at low T an inelastic Lorentzian ($\omega_0 \neq 0$) best describes the ω dependence. Note that in both

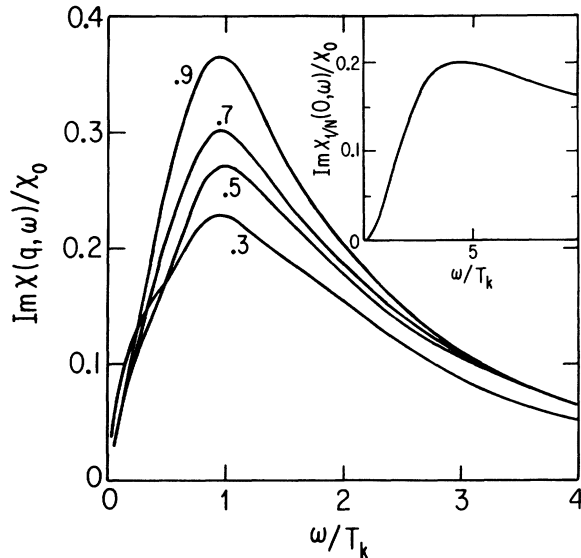


FIG. 1. Frequency dependence of leading-order dynamical susceptibility for various $\mathbf{q}=(0, q, q)$ in units of π/a^* at low k_F (intradband-dominated regime). Curves are normalized to mean-field static susceptibility χ_0 . Inset: $q=0$ results at $T=0$.

cases I and II three dimensionality and umklapp processes "hide" the exact magnitude of the Fermi wave vector so that the relevant momentum scale for the spin correlations is determined by the characteristic rare-earth separation. On the basis of experiments,^{2,3} it seems plausible that case II represents the behavior of CeCu₆, whereas case I may correspond to UPt₃. For realistically complex band structures, both types of contributions might arise from different sheets of the Fermi surface.

(III) For intermediate values of k_F there is a delicate interplay between the interband and intraband terms leading to a nonmonotonic q dependence of the neutron cross section. For most band structures this intermediate regime is rather narrow so that $\text{Im}\chi(q, \omega)$ generally shows an antiferromagnetic peak at the zone-boundary wave vector with $\omega \sim T_K$.

The results for the zone-center susceptibility $\text{Im}\chi(0, \omega)$ are shown in the inset of Fig. 1. [There is also a $\omega\delta(\omega)$ contribution not shown.] For consistency of magnitude we choose $\bar{\mu}=(\chi_0/\gamma)^{1/2}$. As is consistent with Fermi-liquid theory, at low ω $\text{Im}\chi(0, \omega)$ varies as ω^2 ; it has a weak maximum at $\omega \sim 4T_K$ and a high-frequency tail which decays as $\sim \omega^{-1/2}$. Here a fit by a Lorentzian function appears to be inappropriate. Sizable zone-center susceptibilities which are similar to our curve have been observed in neutron single-crystal measurements.²³ It is known that $\text{Im}\chi(0, \omega)$ is accessible to polarized light scattering. Such experiments¹² have recently reported a high-frequency dependence consistent with $\omega^{-1/2}$. It should be stressed that the same energy scale governs the behavior of zone-center and finite- q contributions.

The insets in Fig. 2 focus on fitting procedures and

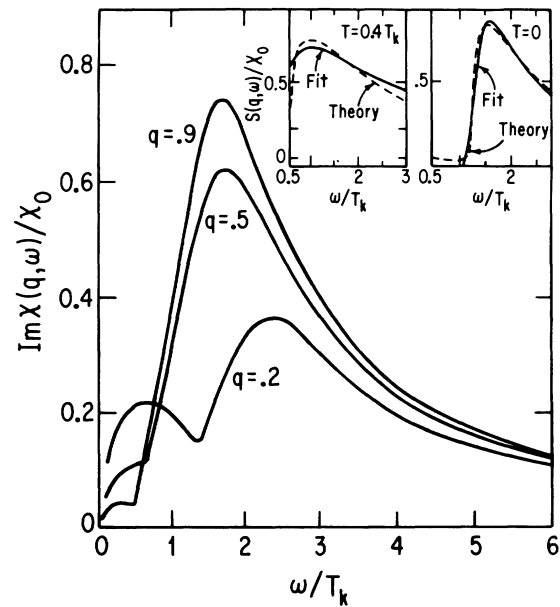


FIG. 2. Frequency dependence of mean-field susceptibility for interband-dominated regime (large k_F). Insets: Theoretical curves (dashed lines) for zone-boundary wave vectors and Lorentzian fits (solid lines) using Eq. (7). The insets demonstrate transitions from inelastic to quasielastic behavior as temperature is slightly raised from $T=0$.

temperature-dependent effects for case II. The temperature dependence of the mean-field parameters can be included into Eq. (2) by use of the same functional form with $T_K(T)=T_K[1+O(T/T_K)^2]$ at sufficiently low $T < T_K/2$. At higher T the entire mean-field approach breaks down.

Thus the role of this T dependence is to rescale the axes and will not affect our general conclusions. Theoretical results for the structure factor $S \equiv \text{Im}\chi(q, \omega)/(1 - e^{-\beta\omega})$ for the same mean-field model as in the main figure are plotted for $\mathbf{q}=(0, 0.9, 0.9)\pi/a^*$ at $T=0.4T_K$ and at $T=0$ (dashed lines) in the insets. Lorentzian fits with Eq. (7) are shown by the solid lines. At the higher temperatures reasonable fits with quasielastic Lorentzians ($\omega_0=0$) are found in both theory and experiment.³ For the lower temperatures, however, it was essential to use *inelastic* Lorentzians. In this case the growing deviations from inelastic to quasielastic Lorentzians as T increases reflect the transition from coherent to incoherent, independent impurity behavior. Similar observations, although with slightly different modified Lorentzians were previously made in analysis of experiments on CeCu₆ reported in Ref. 3. It is interesting to note that in recent CeCu₆ experiments² it was found that the product $\chi_m\Gamma$ is q independent to within 10%. A similar relation is found for our low- T theoretical results.

The general features of Figs. 1 and 2 are in agreement with the data.²⁻⁴ Because we have modeled the conduction-electron dispersion and calculated only

leading-order terms, quantitative comparisons with neutron experiments is not possible. It is expected that the intraband low-frequency structure of Fig. 2 will blend in with the interband terms when Fermi velocity anisotropy and the $1/N$ finite- q corrections are included. A calculation of the $O(1/N)$ corrections at finite q is not feasible. However, since additional internal summations are involved, we estimate a weaker q dependence than in $\text{Im}\chi_{\text{MF}}$. Thus lifetime effects would not alter the basic features of Figs. 1 and 2. Sum-rule arguments have been cited² as experimentally ruling out the existence of intraband terms. However, on the basis of other measurements (e.g. de Haas-van Alphen data⁷), these Fermi-liquid effects are expected to be present although partially obscured by nuclear scattering.

The role of antiferromagnetic spin fluctuations on the superconductivity is at the heart of current interest in heavy fermions as well as in the new high- T_c superconductors. This issue can be addressed at two levels:

(1) In the context of the $1/N$ expansion, resummation scheme is a required to treat the superconductivity. The antiferromagnetic fluctuations which have been discussed above do not appear in the leading-order direct vertex function Γ which, like the phonon case, does not involve a spin-spin coupling $\mathbf{S}\cdot\mathbf{S}$. As a consequence in the simplest resummation scheme⁵ these antiferromagnetic fluctuations do not directly mediate the superconductivity.

(2) In the context of more phenomenological approaches^{13,14} it is assumed that $\Gamma \propto \chi \mathbf{S}\cdot\mathbf{S}$. By contrast with nearly magnetic Fermi liquids (e.g., ³He), the characteristic spin-fluctuation frequencies in χ are not "soft" but rather comparable to the quasiparticle energies. This calls into question Fermi-liquid and weak-coupling-type approaches¹³ for calculating T_c , and raises the issue of whether these highly inelastic fluctuations (which do not correlate with the occurrence of superconductivity as seen, e.g., in CeCu₆) dominate the pairing interaction. In the theory of Ref. 14 other conditions besides the mere existence of these fluctuations are necessary to obtain a superconducting state. Note that these fluctuations are to be distinguished from true spin-density-wave order. The $1/N$ formulation can be extended to include these effects by invocation of resummation schemes in the particle-hole channels.

Since we predict that the characteristic neutron-scattering peaks scale with $T_k \propto \gamma^{-1}$, studies of pressure effects as well as systematic correlations in different compounds would be most interesting. The currently available neutron data yield estimates of $T_K \approx 30$ K and 2–10 K for UPt₃ (Ref. 2) and CeCu₆ (Refs. 2,3), respectively. Resistivity and specific-heat measurements^{15,16} on UPt₃ suggest that $T_K \approx 15$ –40 K, whereas similar measurements¹⁶ on CeCu₆ yield 4–7 K.

We thank G. Aeppli, B. Brandow, and A. J. Leggett for useful suggestions. This work was supported by National Science Foundation Grants No. DMR 84-20187 and No. NSF-MRL-DMR-16892 and U.S. Department

of Energy Grant No. US-DOE W-31-109-ENG-38. We acknowledge receipt of National Science Foundation supercomputer funds.

¹A. Auerbach and K. Levin, Phys. Rev. B **34**, 3524 (1986), and J. Appl. Phys. **61**, 3162 (1987), and references therein.

²G. Aeppli *et al.*, Phys. Rev. Lett. **58**, 808 (1987); G. Aeppli *et al.*, Phys. Rev. Lett. **57**, 122 (1986).

³L. P. Regnault *et al.*, J. Magn. Magn. Mater. **63–64**, 289 (1987).

⁴K. U. Neumann *et al.*, Solid State Commun. **60**, 641 (1986). These measurements at 10 K were above the onset of coherence of UBe₁₃ ($T \approx 2$ K).

⁵A. Auerbach and K. Levin, Phys. Rev. Lett. **57**, 877 (1986); A. J. Millis and P. A. Lee, Phys. Rev. B **35**, 3394 (1987), and references therein.

⁶C. J. Pethick and D. Pines, in *Novel Superconductivity*, edited by S. A. Wolf and V. Z. Kresin (Plenum, New York, 1987), p. 201.

⁷See, for example, L. Taillefer *et al.*, J. Magn. Magn. Mater. **63–64**, 372 (1987).

⁸Z. Zou and P. W. Anderson, Phys. Rev. Lett. **57**, 2073 (1986); F. C. Zhang and T. K. Lee, Phys. Rev. B **35**, 3657 (1987). Importance of crystal-field effects was pointed out by D. L. Cox, Phys. Rev. Lett. **58**, 2730 (1987). These effects enter through the decomposition $|m\rangle = \sum_{\mu} a_{\mu}^m |\frac{5}{2}, \mu\rangle$ where $|J, \mu\rangle$ are angular momentum states and a_{μ}^m depend on crystal symmetries. The lowest doublets are for CeCu₆: $|\pm\rangle = (1/6)^{1/2} |\frac{5}{2}, \pm \frac{3}{2}\rangle + (5/6)^{1/2} |\frac{5}{2}, \pm \frac{1}{2}\rangle$. For UPt₃, based on susceptibility anisotropy, we estimate $|\pm\rangle = |\frac{5}{2}, \pm \frac{1}{2}\rangle$ (Γ^8).

⁹Fermi-liquid properties of Eq. (1) do not differ significantly from those calculated in Ref. 5, although field-dependent (e.g., magnetotransport) coefficients depend on the details of the crystal-field structure.

¹⁰This behavior arises because μ [see Ref. (8)] depends primarily on the direction of \mathbf{k} (through Y_{3m}). At small q , $\text{Im}\bar{\Pi} \sim q^2$, and at larger q it is dominated by interband transitions which behavior is approximated by our simple exponential function.

¹¹Similar observations for mixed valence compounds were made by A. J. Fedro and S. K. Sinha, in *Valence Fluctuations in Solids*, edited by L. M. Falikov, W. Hanke, and M. B. Maple (North-Holland, New York, 1981); D. L. Huber, Phys. Rev. B **28**, 860 (1983). For heavy fermions: B. H. Brandow, to be published; A. Auerbach and K. Levin, Bull. Am. Phys. Soc. **32**, 594 (1987).

¹²L. S. Cooper *et al.*, in *Proceedings of the Eighteenth Yamada Conference on Superconductivity in Highly Correlated Fermion Systems, Sendai, Japan, 1987* (North-Holland, Amsterdam, 1987).

¹³K. Miyake, S. Schmitt-Rink, and C. M. Varma, Phys. Rev. B **34**, 6554 (1986); D. J. Scalapino, E. Loh, and J. E. Hirsch, Phys. Rev. B **34**, 8190 (1986).

¹⁴M. R. Norman, Phys. Rev. Lett. **59**, 232 (1987).

¹⁵A thorough review of UPt₃ is found in A. de Visser, Ph.D. thesis, 1986 (unpublished).

¹⁶J. D. Thompson, in *Proceedings of the International Conference on Anomalous Rare Earths and Actinides, Grenoble, France, 1986*, edited by J. X. Boucherle *et al.* (North-Holland, Amsterdam, 1987).